Estimation of Impedance Ratio Parameters for Consistent Modeling of Tap-Changing Transformers

Md Rejwanur R. Mojumdar, *Graduate Student Member, IEEE*, José M. Cano, *Senior Member, IEEE*, and Gonzalo A. Orcajo, *Member, IEEE*

***Abstract*—Recent contributions have shown that two widely used formulations of the tap-changing transformer model are controversial, as they generate dissimilar results depending on the selected tap and operating point. In recent works, the authors proposed a new model and demonstrated its consistency to reconcile this debate. It introduces a parameter which stands for the ratio between the impedances of the nominal and tapped winding of the transformer. However, this parameter is not provided with and cannot be obtained from standard datasheets, which compels the users to rely on rough approximations. To overcome this problem, an offline state-vector-augmented parameter estimation method capable of providing accurate estimates of transformer impedance ratios is proposed in this work. It is demonstrated that their use can effectively lead state estimators to better estimates of system states. This work also contributes with the derivatives of the different measurement functions in terms of the impedance ratios, which are essential for this or any other linearized state estimator. A multi-snapshot implementation is used to obtain a twofold advantage — increased measurement redundancy and improved accuracy of the estimated parameters. A detailed formulation of the implementation and several case studies are presented to demonstrate the validity of the proposal.**

***Index Terms*—Maximum likelihood estimation, parameter estimation, power transformers, tap changers, transformer models.**

I. Introduction

SEVERAL power system studies, such as power flow (PF), optimal power flow (OPF) or state estimation (SE), are crucial today to ensure safety and optimality in the operation of modern grids. In this context, tap-changing transformers serve at the vanguard for voltage regulation in power systems, and thus, accurate models of these devices are needed when they are present in the network under study.

The two most widely spread tap-changing transformer models found both in literature and software packages [1], [2] have been demonstrated to be inconsistent [3]–[5]. One of the models assumes that the transformer impedance, obtained through the well-known short-circuit test, is totally provided by the nominal winding, whereas the other model allocates it exclusively at the off-nominal side. This fact was first reported in [3]; however, the authors of this work selected one of the alternatives and proposed a method to shape the other so as to converge into the same results. Later, in [4], [5], it was established that, while the two models produce similar results near the central tap, they lead to significant differences at extreme tap positions. The power factor of the power flowing through the transformer primarily determines whether this divergence appears in voltage magnitude or phase angle. Analytical formulations and case studies demonstrating this inconsistency are presented in the aforementioned references.

To reconcile this dispute, the authors proposed a consistent model which reflects that the short-circuit impedance is in fact shared by both sides of the transformer [4], [5]. The new model introduces a parameter, k, which stands for the per-unit (p.u.) impedance ratio between the nominal winding and tapped winding of the tap-changing transformer. However, admittedly, the user cannot obtain the value of this parameter from standard transformer data sheets or even through straight-forward calculations. In response to that, the authors argued and demonstrated that if this parameter is not available, assuming $k = 1$, i.e. considering an equal share of the p.u. impedance at both sides of the transformer, produces results which minimizes the maximum expected error. Nonetheless, the authors pointed out that, to achieve accurate results, the p.u. impedance ratio could be obtained in real scenarios from the application of SE techniques. In fact, this is the main purpose of the present proposal.

In a broad classification, SE methods are either recursive or static. However, static state estimators constitute a comparatively mature technology widely used by utilities for power system monitoring. While there are other possibilities, most of the static estimators minimize the weighted least squares (WLS) of residuals from a single snapshot of measurements to provide estimates of the current states of the system [6], [7]. For static SE, several alternative formulations are available in literature in order to overcome some deficiencies of the seminal algorithms, increasing numerical capabilities or adding some practical advantages. Many of these formulations are well documented in [6], [7]. In the present proposal, a widely used and suitable WLS-based formulation is extended further to cope with the objectives of this work.

Manuscript received June 3, 2020; revised October 16, 2020 and December 24, 2020; accepted January 2, 2021. Date of publication January 12, 2021; date of current version June 18, 2021. This work was supported by the Spanish Government Innovation Development, and Research Office (MEC) under research Grant DPI2017-89186-R. Paper no. TPWRS-00922-2020. *(Corresponding author: José M. Cano.)*

Md Rejwanur R. Mojumdar is with the Electrical Control System Department, ABB AS, 4033 Stavanger, Norway (e-mail: rejwanurrashid.mojumdar@no.abb.com).

José M. Cano and Gonzalo A. Orcajo are with the Department of Electrical Engineering, University of Oviedo, 30013 Gijón, Spain (e-mail: jmcano@uniovi.es; gonzalo@uniovi.es).

Color versions of one or more figures in this article are available at https://doi.org/10.1109/TPWRS.2021.3050958.

Digital Object Identifier 10.1109/TPWRS.2021.3050958

In addition to providing estimates of the state variables, other functions and associated routines are integral parts of power system state estimators, such as observability analysis, bad data detection and identification, topology error processing and parameter estimation. Among these, the latter can be pointed out as the key tool to address the problem of estimating the p.u. impedance ratios of tap-changing transformers. Network parameter estimation methods are broadly classified in two groups-residual sensitivity-based analysis and state vector augmentation [6]. Residual sensitivity-based analysis is efficient for parameter error identification which is not required for the purpose of this work, as transformer impedance ratios are objectively included in the suspicious set. As the name suggests, in state vector augmentation methods, the suspected parameters are included in the state vector and estimated together with the system state variables [8]–[13]. Importantly, for the sole purpose of parameter estimation, state vector augmentation methods are considered to deliver superior performance due to the fact that all the surrounding measurements get involved in the estimation [14]. Therefore, the state vector augmentation method has been selected and implemented in this proposal to provide accurate estimates of the parameters of interest.

The estimation of transformer tap positions has been a central issue for parameter estimation methods in power systems [10], [13]. In fact, estimation of unmeasured or erroneous transformer taps is today a regular or online function of state estimators. On the contrary, due to the non-varying nature of impedance ratio parameters, which may change only in the event of a fault or a complete replacement of a transformer, their estimation is required in very long intervals. It is not worth including the estimation of these parameters in an online state estimator, as this may deteriorate the performance of the algorithm in terms of speed without a practical improvement. Therefore, an offline parameter estimator, designed to be run periodically, with a low cadence, is proposed in this work. In this concept, the online estimator used in the operation of the grid is in charge of the estimation of transformer tap positions at each snapshot; then, the offline parameter estimator, executed in long time periods, uses those tap positions together with the raw measurements at different snapshots to provide accurate estimates of the transformer impedance ratios. Certainly, the updated estimates of these parameters can now be fed into the online state estimator to increase its accuracy, as a consequence of the improvement of the model.

Finally, it is important to discuss the potential hindrances of assessing the transformer p.u. impedance ratios through parameter estimation techniques. If a large number of tap-changing transformers are embedded in the grid under study, the new variables to be included in the augmented state vector could significantly deteriorate the redundancy of the measurements. Moreover, as in any other SE application, the noise of field measurements has an impact on the quality of the estimation of the parameters. However, even more important for this particular problem is that the sensitivity of the measurement functions with respect to p.u. impedance ratios are significantly lower than the sensitivities with respect to the other state variables. As a consequence, measurement noise is likely to conceal the biases of erroneous estimation of impedance ratios throughout the process. The above-mentioned difficulties turn the estimation of the desired transformer parameters into a challenging task. Nonetheless, one expedient feature of transformer impedance ratios can help to overcome these obstacles: they can be considered time-invariant, at least for a reasonable time span. Thus, the method proposed in this work can be fed with multiple snapshots of measurements, i.e. with historical data collected along a reasonable time period. Multi-snapshots usage has clear advantages in parameter estimation, as has been previously reported by other authors [6], [9], [11]. Therefore, a multi-snapshot implementation has been embraced in this proposal.

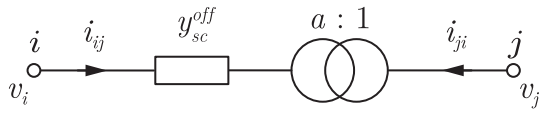

Fig. 1. Model of the tap-changing transformer with short-circuit impedance at the off-nominal turns side.

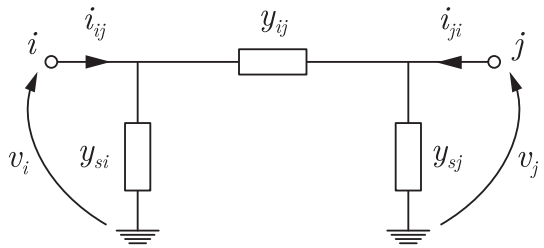

Fig. 2. Two-port π-model of a tap-changing transformer or a network branch.

In Section II, the consistent tap-changing transformer model, and thereby, the emergence of the impedance ratio parameter, is presented for the benefit of the reader. Then, an advantageous equality-constrained SE method is briefly described in Section III. Section IV articulates the derivation and integration details of the estimation of p.u. impedance ratios. A set of case studies are included in Section V to validate and demonstrate the advantages of the proposal. Finally, the conclusions of this study are gathered in Section VI.

II. Consistent Tap-Changing Transformer Model

Let us consider a tap-changing transformer with off-nominal turns ratio $a:1$ as depicted in Fig. 1. Like any network branch or in-phase transformer, a tap-changing transformer can be represented as a π-equivalent model, as shown in Fig. 2. The π-equivalent model possesses two shunt branches which induce no effect while the transformer is operated at its nominal turns ratio. However, tap-changing transformers are often operated at off-nominal turn ratios for voltage regulation purposes, and thus, the shunt branches of their π-equivalent model cannot be neglected.

As discussed in Section I, the consistent model of the tap-changing transformer was introduced in [4], [5] to reconcile the inconsistency between two widespread models. The new consistent model states that the off-nominal short-circuit admittance

at the off-nominal turns side can be calculated as

$$y_{sc}^{off} = \frac{1}{z_1 + a^2 z_2} = \frac{1+k}{1+ka^2} y_{sc}, \tag{1}$$

where y_{sc} represents the p.u. admittance of the transformer, obtained through the short-circuit test and always provided as nameplate data. Parameter k is introduced in [4] to denote the p.u. impedance ratio between the nominal winding, z_2, and tapped winding, z_1. Classical transformer models assume extreme values of this parameter ($k = 0$ and $k = \infty$). The elements of the bus admittance matrix for the consistent tap-changing transformer model are derived in [4], [5] as

$$Y_{ii} = \frac{1+k}{1+ka^2} y_{sc}, \tag{2}$$

$$Y_{ij} = Y_{ji} = -\frac{a(1+k)}{1+ka^2} y_{sc}, \tag{3}$$

$$Y_{jj} = \frac{a^2(1+k)}{1+ka^2} y_{sc}. \tag{4}$$

Then, the parameters of the π-model can be straightforwardly obtained as

$$y_{ij} = -Y_{ij} = \frac{a(1+k)}{1+ka^2} y_{sc}, \tag{5}$$

$$y_{si} = Y_{ii} + Y_{ij} = \frac{(1-a)(1+k)}{1+ka^2} y_{sc}, \tag{6}$$

$$y_{sj} = Y_{jj} + Y_{ij} = \frac{a(a-1)(1+k)}{1+ka^2} y_{sc}. \tag{7}$$

An unresolved issue of the consistent model is that the particular value of the p.u. impedance ratio, k, for a specific tap-changing transformer is a constructive parameter normally unknown for the user. Therefore, the accuracy and consistency of the results of power system studies with embedded tap-changing transformers can be obviously improved if the actual value of k is determined through a parameter estimation process utilizing historical sets of measurements. Thus, the estimation of k is pursued in the present proposal.

III. Equality-Constrained SE

The Normal Equations (NE) formulation of WLS SE in their application to power system studies may lead to some well-known problems, such as ill-conditioning or divergence. This is especially critical when using zero-injection buses as virtual measurements. Therefore, several proposals have been made to overcome the shortcomings of the basic NE formulation [6]. Among these propositions, appear numerical techniques such as the Lower Upper (LU) factorization and orthogonal (QR) factorization of the gain matrix. More advantageously, there are some restructured formulations called equality-constrained SE which take advantage of the Lagrangian of equality-constrained optimization problems [6], [15]. In the present work, an equality-constrained SE algorithm called augmented matrix method [6], [16] was extended to the particular parameter estimation problem of interest. In this method, both the virtual and regular measurement equations are taken as equality constraints in order to improve the condition number of the Hachtel's matrix. According to this method, the following set of linearized equations describes the SE problem

$$\begin{bmatrix} R & H & 0 \\ H^T & 0 & C^T \\ 0 & C & 0 \end{bmatrix} \begin{bmatrix} \mu \\ \Delta x \\ \lambda \end{bmatrix} = \begin{bmatrix} \Delta z \\ 0 \\ -c(x) \end{bmatrix}, \tag{8}$$

where,

- R is the covariance matrix having variances of regular measurement errors at its diagonal elements,
- H is the matrix for derivatives of regular measurements,
- C is the matrix for derivatives of virtual measurements,
- μ is the vector of Lagrange multipliers for regular measurements,
- λ is the vector of Lagrange multipliers for virtual measurements,
- Δx is the vector for deviations of state variables,
- Δz is the vector for measurement residuals, i.e., the difference between regular field measurements and their theoretical values calculated from the current estimation of state variables,
- and $c(x)$ is the vector for virtual measurement residuals.

IV. Estimation of Transformer Impedance Ratios

Most SE methods are linearized formulations which require the derivatives of the measurement functions, h, in terms of the state variables. As power system static SE is a well-developed and mature technique, the derivatives of general measurement functions in terms of commonly used state variables and parameters are widely used and readily available in the literature [6]. However, the consistent tap-changing transformer model is a state-of-the-art concept which has not been implemented before in power system SE algorithms. Hence, no work has yet introduced the derivatives of measurement functions in terms of the impedance transformer ratio, k, which are required for the estimation of these parameters.

In a standard SE formulation, the state vector, x, includes bus voltage magnitudes, V, and phase angles, θ, except for the phase angle reference, as state variables. In this proposal, the state vector is augmented by including the k parameters of the tap-changing transformers embedded in the network under study. Thus, as an important contribution of this work, the derivatives of general field measurement types such as bus voltage magnitudes, active and reactive bus power injections and active and reactive branch power flows, in terms of the impedance ratio, are presented. These derivatives are crucial for the construction of both the H and C matrices included in (8). Finally, for the problem-specific requirements, the authors have integrated these new derivatives into a single snapshot and a multi-snapshot augmented matrix SE algorithm.

A. Derivatives of Measurement Functions in Terms of k

1) Bus Voltage Magnitudes: The measurement function of voltage magnitude at bus i reduce itself to its corresponding voltage magnitude, V_i, which is a state variable on its own.

Therefore, these functions are independent of tap-changing transformer impedance ratios, k. So, it can be stated that

$$\frac{\partial V_i}{\partial k} = 0. \tag{9}$$

2) Power Injections: The measurement functions for the active and reactive power injections, P_i and Q_i, at a specific bus i, are well-known in power system analysis, being formulated as

$$P_i = V_i \sum_{n=1}^{N} V_n [G_{in} \cos\theta_{in} + B_{in} \sin\theta_{in}], \tag{10}$$

$$Q_i = V_i \sum_{n=1}^{N} V_n [G_{in} \sin\theta_{in} - B_{in} \cos\theta_{in}], \tag{11}$$

where n stands for each of the total number of buses in the network, N. Likewise, G_{in}, B_{in} are the conductance and susceptance of the element Y_{in} of the system bus admittance matrix. Finally, θ_{in} stands for the phase angle between buses i and n.

As it can be immediately concluded from (10) and (11), if bus i is not directly connected to a tap-changing transformer, none of the terms of these equations depend on the impedance ratio of that specific device. Thus, the derivatives of those active and reactive power injections in terms of the impedance ratio of that transformer equal zero. On the other hand, if there is a tap-changing transformer located between buses i and j, with an impedance ratio k, the admittance of the transformer impacts the calculation of power injections through the addends corresponding to $n = i$ and $n = j$. Thus, the parts of P_i and Q_i impacted by k, which are the only ones of interest for the calculation of the derivatives, can be designated as P_i^k and Q_i^k and may be evaluated as

$$P_i^k = V_i^2 G_{ii}^k + V_i V_j [G_{ij} \cos\theta_{ij} + B_{ij} \sin\theta_{ij}], \tag{12}$$

$$Q_i^k = -V_i^2 B_{ii}^k + V_i V_j [G_{ij} \sin\theta_{ij} - B_{ij} \cos\theta_{ij}], \tag{13}$$

where, G_{ii}^k and B_{ii}^k contain the addends of the diagonal elements of the bus admittance matrix which are a function of k, i.e. those provided by the series and shunt branch of the tap-changing transformer model connected at bus i.

At this point, two cases should be taken into consideration. On the one hand, if the tapped winding of the transformer is connected to bus i, as depicted in Fig. 1, (2) and (3) allow to express the elements of the bus admittance matrix in (12) and (13) as a function of k and the conductance, g_{sc}, and susceptance, b_{sc}, of the short-circuit admittance, y_{sc}, of the transformer. Thus,

$$G_{ii}^k = \frac{1+k}{1+ka^2} g_{sc}, \qquad B_{ii}^k = \frac{1+k}{1+ka^2} b_{sc}, \tag{14}$$

$$G_{ij} = -\frac{a(1+k)}{1+ka^2} g_{sc}, \quad B_{ij} = -\frac{a(1+k)}{1+ka^2} b_{sc}. \tag{15}$$

The substitution of (14) and (15) in (12) and (13) leads to

$$P_i^k = \frac{1+k}{1+ka^2} \left[V_i^2 g_{sc} - a V_i V_j \left(g_{sc} \cos\theta_{ij} + b_{sc} \sin\theta_{ij} \right) \right], \tag{16}$$

$$Q_i^k = \frac{1+k}{1+ka^2} \left[-V_i^2 b_{sc} - a V_i V_j \left(g_{sc} \sin\theta_{ij} - b_{sc} \cos\theta_{ij} \right) \right]. \tag{17}$$

By applying the quotient rule to (16) and (17), the derivatives of P_i and Q_i in terms of k can be obtained as

$$\frac{\partial P_i}{\partial k} = \frac{1+ka^2-a^2(1+k)}{(1+ka^2)^2} \times \ldots \left[V_i^2 g_{sc} - a V_i V_j \left(g_{sc} \cos\theta_{ij} + b_{sc} \sin\theta_{ij} \right) \right], \tag{18}$$

$$\frac{\partial Q_i}{\partial k} = \frac{1+ka^2-a^2(1+k)}{(1+ka^2)^2} \times \ldots \left[-V_i^2 b_{sc} - a V_i V_j \left(g_{sc} \sin\theta_{ij} - b_{sc} \cos\theta_{ij} \right) \right]. \tag{19}$$

On the other hand, if bus i is connected to the untapped winding of the transformer, (4) should be used instead of (2) to formulate the diagonal elements of the bus admittance matrix impacted by k, G_{ii}^k and B_{ii}^k, in (12) and (13). Thus,

$$G_{ii}^k = \frac{a^2(1+k)}{1+ka^2} g_{sc}, \quad B_{ii}^k = \frac{a^2(1+k)}{1+ka^2} b_{sc}. \tag{20}$$

The substitution of (15) and (20) in (12) and (13) leads to

$$P_i^k = \frac{a(1+k)}{1+ka^2} \left[a V_i^2 g_{sc} - V_i V_j \left(g_{sc} \cos\theta_{ij} + b_{sc} \sin\theta_{ij} \right) \right], \tag{21}$$

$$Q_i^k = \frac{a(1+k)}{1+ka^2} \left[-a V_i^2 b_{sc} - V_i V_j \left(g_{sc} \sin\theta_{ij} - b_{sc} \cos\theta_{ij} \right) \right]. \tag{22}$$

And the derivatives of P_i and Q_i in terms of k in this second case turn out to be

$$\frac{\partial P_i}{\partial k} = \frac{a(1+ka^2)-a^3(1+k)}{(1+ka^2)^2} \times \ldots \left[a V_i^2 g_{sc} - V_i V_j \left(g_{sc} \cos\theta_{ij} + b_{sc} \sin\theta_{ij} \right) \right], \tag{23}$$

$$\frac{\partial Q_i}{\partial k} = \frac{a(1+ka^2)-a^3(1+k)}{(1+ka^2)^2} \times \ldots \left[-a V_i^2 b_{sc} - V_i V_j \left(g_{sc} \sin\theta_{ij} - b_{sc} \cos\theta_{ij} \right) \right]. \tag{24}$$

3) Power Flows: Note that the π-equivalent model depicted in Fig. 2 is not only valid for a tap-changing transformer but also for a line. Thus, the measurement functions of active and reactive power, P_{ij}, Q_{ij}, flowing from bus i to bus j and measured at the sending end can be expressed for both types of elements as

$$P_{ij} = V_i^2 (g_{si} + g_{ij}) - V_i V_j (g_{ij} \cos\theta_{ij} + b_{ij} \sin\theta_{ij}), \tag{25}$$

$$Q_{ij} = -V_i^2 (b_{si} + b_{ij}) - V_i V_j (g_{ij} \sin\theta_{ij} - b_{ij} \cos\theta_{ij}), \tag{26}$$

where, g_{si} and b_{si} are the conductance and susceptance of the shunt leg at bus i, and g_{ij} and b_{ij} stand for the conductance and susceptance of the series admittance.

From (25) and (26), it can be immediately concluded that, if a power flow measurement between the adjacent buses i and j does not flow through a tap-changing transformer, none of the elements of these equations are affected by the impedance ratio of the device. Thus, the derivatives of those active or reactive power flows in terms of the k equal zero. However, when a tap-changing transformer connects buses i and j, the admittances in those equations are a function of the impedance ratio, k. Again, two different cases need to be addressed. On the one hand, if the measuring location, i.e. bus i, is connected to the tapped winding, as in Fig. 1, the conductances and susceptances can be directly taken from (5) and (6). Thus,

$$g_{si} + g_{ij} = \frac{1+k}{1+ka^2} g_{sc}, \qquad b_{si} + b_{ij} = \frac{1+k}{1+ka^2} b_{sc}, \quad (27)$$

$$g_{ij} = \frac{a(1+k)}{1+ka^2} g_{sc}, \qquad b_{ij} = \frac{a(1+k)}{1+ka^2} b_{sc}. \quad (28)$$

The substitution of (27) and (28) in (25) and (26) leads to

$$P_{ij} = \frac{1+k}{1+ka^2} \left[V_i^2 g_{sc} - a V_i V_j \left(g_{sc} \cos\theta_{ij} + b_{sc} \sin\theta_{ij} \right) \right], \quad (29)$$

$$Q_{ij} = \frac{1+k}{1+ka^2} \left[-V_i^2 b_{sc} - a V_i V_j \left(g_{sc} \sin\theta_{ij} - b_{sc} \cos\theta_{ij} \right) \right]. \quad (30)$$

By applying the quotient rule to (29) and (30), the derivatives of P_{ij} and Q_{ij} in terms of k can be obtained as

$$\frac{\partial P_{ij}}{\partial k} = \frac{1+ka^2-a^2(1+k)}{(1+ka^2)^2} \times \ldots \left[V_i^2 g_{sc} - a V_i V_j \left(g_{sc} \cos\theta_{ij} + b_{sc} \sin\theta_{ij} \right) \right], \quad (31)$$

$$\frac{\partial Q_{ij}}{\partial k} = \frac{1+ka^2-a^2(1+k)}{(1+ka^2)^2} \times \ldots \left[-V_i^2 b_{sc} - a V_i V_j \left(g_{sc} \sin\theta_{ij} - b_{sc} \cos\theta_{ij} \right) \right]. \quad (32)$$

On the other hand, if the measuring location, i.e. bus i, is connected to the untapped winding, (7) should be used instead of (6) to obtain the conductances and susceptances used in (29) and (30). Thus,

$$g_{si} + g_{ij} = \frac{a^2(1+k)}{1+ka^2} g_{sc}, \quad b_{si} + b_{ij} = \frac{a^2(1+k)}{1+ka^2} b_{sc}. \quad (33)$$

The substitution of (28) and (33) in (29) and (30) leads to

$$P_{ij} = \frac{a(1+k)}{1+ka^2} \left[a V_i^2 g_{sc} - V_i V_j \left(g_{sc} \cos\theta_{ij} + b_{sc} \sin\theta_{ij} \right) \right], \quad (34)$$

$$Q_{ij} = \frac{a(1+k)}{1+ka^2} \left[-a V_i^2 b_{sc} - V_i V_j \left(g_{sc} \sin\theta_{ij} - b_{sc} \cos\theta_{ij} \right) \right]. \quad (35)$$

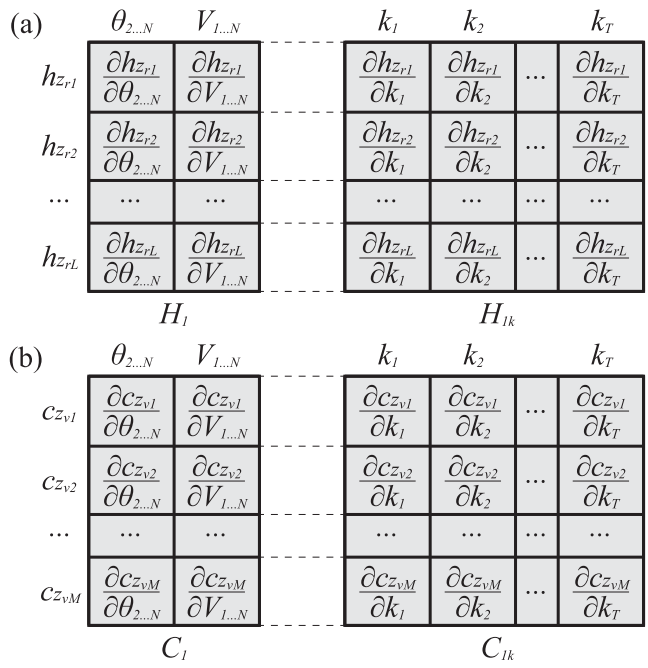

Fig. 3. Formation of the augmented Jacobian matrices for a single snapshot. (a) H matrix, and (b) C matrix.

And the derivatives of P_{ij} and Q_{ij} in terms of k in this second case can be expressed as

$$\frac{\partial P_{ij}}{\partial k} = \frac{a(1+ka^2)-a^3(1+k)}{(1+ka^2)^2} \times \ldots \left[a V_i^2 g_{sc} - V_i V_j \left(g_{sc} \cos\theta_{ij} + b_{sc} \sin\theta_{ij} \right) \right], \quad (36)$$

$$\frac{\partial Q_{ij}}{\partial k} = \frac{a(1+ka^2)-a^3(1+k)}{(1+ka^2)^2} \times \ldots \left[-a V_i^2 b_{sc} - V_i V_j \left(g_{sc} \sin\theta_{ij} - b_{sc} \cos\theta_{ij} \right) \right]. \quad (37)$$

B. Formation of Jacobian Matrices for the SE Process

In the formulation of the augmented matrix approach for SE [6], [15], the derivatives of the h_z–functions of a set of L regular measurements, z_r, reside in the H matrix, while the derivatives of the c_z–functions of a set of M virtual measurements, z_v, reside in the C matrix shown in (8). Both matrices are augmented in this proposal with a new set of state variables, k, corresponding to the transformer impedance ratios of the T tapped-transformers embedded in the grid under study.

If the estimation of k is carried out considering just a single snapshot of measurements, the extension of the Jacobian matrices is rather straightforward. In this case, a new column has to be added, both to the H and C matrices, to account for each of the T elements of k. Thus, the use of the new derivatives described in Section IV-A together with the classical set [6], allows to form the augmented H and C matrices as depicted in Fig. 3. Notice that in this figure and w.l.o.g, the phase angle at bus 1, θ_1, has been taken as reference, and thus, excluded from the set of

state variables. This is a similar approach to other augmentation techniques such as those previously presented in [8]–[13].

According to Fig. 3, two parts can be distinguished in the new H and C matrices: H_1 and C_1, that account for the derivatives of regular and virtual measurements with respect to the conventional state variables, and H_{1k} and C_{1k}, that hold the derivatives of regular and virtual measurements in terms of the transformer impedance ratios, k. The final H and C matrices are formed by horizontal concatenation of H_1, H_{1k} and C_1, C_{1k} respectively.

The difficulties of estimating the p.u. impedance ratios of tap-changing transformers from a single snapshot of measurements have been previously discussed in Section I. As it was pointed out, an adaptation of a multi-snapshot of measurements is proposed in this work to overcome those obstacles. This is a suitable approach for the estimation of the parameters under study, which can be considered time-invariant during long periods. Indeed, parameter estimation, conducted as an offline task, can sacrifice computation time in favor of the accuracy of the estimation.

In SE theory, measurement redundancy is defined as the ratio between the number of measurements and the number of state variables. Hence, as L is the number of regular measurements and M is the number of virtual measurements, the base case redundancy of the problem, ε_0, i.e., the one in which p.u. impedance ratios are not included as state variables, can be calculated as

$$\varepsilon_0 = \frac{L+M}{2N-1}. \tag{38}$$

In a single snapshot or multi-snapshot implementation of the augmented problem, in which Q snapshots and T time-invariant transformer impedance ratios are included as additional state variables, the redundancy level is deteriorated according to

$$\varepsilon_Q = \frac{Q(L+M)}{Q(2N-1)+T} = \frac{L+M}{2N-1+\frac{T}{Q}}. \tag{39}$$

From (39), it can be concluded that, increasing the number of snapshots in the estimation process, allows to move the redundancy level of the augmented problem as close as desired to the redundancy of the base case. Thus, provided that a sufficient number of snapshots are included into the problem, the application of the augmented approach cannot be blamed for deteriorating the redundancy level.

The formation of the augmented matrices, H and C, for the case of the multi-snapshot problem is depicted in Fig. 4. Each snapshot q involves a specific set of conventional state variables, $[V\theta]_q$, together with a specific set of h–functions, $[h_{zr}]_q$, and c–functions, $[c_{zv}]_q$, associated with regular and virtual measurements, respectively. Notice that the conventional state variables change at each snapshot but the augmented ones, k, remain always the same. Thus, the parts of the Jacobian matrices linked to conventional state variables are augmented diagonally by means of H_q and C_q, while the parts associated with the transformer impedance ratios are augmented vertically by means of H_{qk} and C_{qk}.

It is worth noting that, in order to apply (8) in the multisnapshot context, the covariance matrix, R, should be formed by diagonal augmentation of the respective covariance matrices of each snapshot. Likewise, Δz and Δx vectors are respectively formed by vertical concatenation of measurement residuals and state variable deviations from each snapshot.

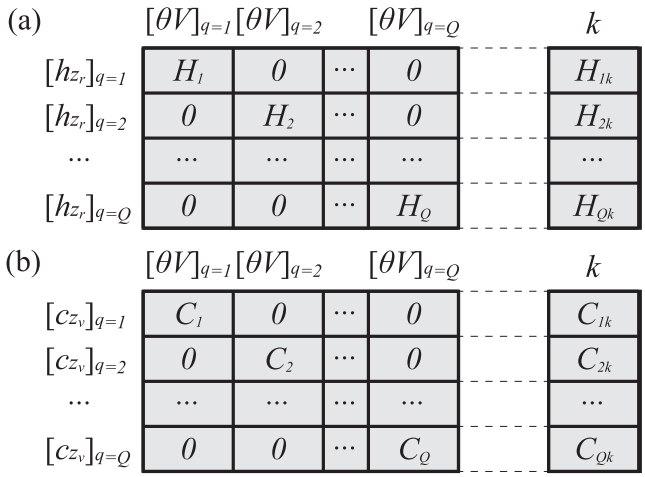

Fig. 4. Formation of the augmented Jacobian matrices in a multi-snapshot problem. (a) H matrix, and (b) C matrix.

Equation (8) can now be iteratively solved to provide estimates of the full set of state variables. Among them, the final values of k constitute the estimated parameters of the p.u. impedance ratios of the tap-changing transformers.

C. Treatment of Bad Data

The treatment of bad data is a crucial concern for any state estimator. However, as it is pointed out in Section I, the parameter estimator proposed in this work is designed to work offline. Thus, it uses historical data comprised of measurement snapshots in which any possible bad data has been already detected, identified and removed by the online state estimator used in the operation of the grid. Of course, removal of bad data may reduce the redundancy of the measurement set. However, as it is shown in the case studies presented in Section V, the proposed algorithm converges to the solution even in low redundancy scenarios. In summary, as the bad data is pre-treated by the online state estimator, the proposed offline parameter estimator does not need further filtering of the input measurements.

Nevertheless, it is interesting to point out that model inaccuracies, such as those that may appear during the initialization process (i.e. when $k = 1$ is adopted as an educated guess of the transformer impedance ratios), can lead the online state estimator to an undesired removal of measurements (erroneously flagged as bad data). The influence of this aspect on the proper estimation of the parameters is studied in Section V-E.

D. Initialization and Pseudomeasurement Strategy

The initialization of the iterative process presented in (8) is conducted considering a flat profile, i.e. all the bus voltage magnitudes are set to 1 p.u. and all the bus voltage phase angles are set to 0 deg. For the case of transformer impedance ratios, k, they are set to 1, which is a sensible educated guess according to [4].

Nonetheless, once the algorithm has been run for the first time in a particular grid, the initialization of the transformer impedance ratios can be changed to adopt the estimated parameters provided as an output by the last execution.

As it is analysed in Subsection IV-B, adding new elements to the state vector reduces measurement redundancy. To counteract this fact, a general practice was common in parameter estimation methods: the inclusion of the last available estimates of the suspicious parameters as pseudomeasurements in the problem. This practice can be applied to the case of the estimation of transformer impedance ratios; however, this strategy has been argued as controversial [6], [14]. Certainly, if the system is not observable without the pseudomeasurements, then the parameters become critical and their estimates become equal to the initialization values. On the other hand, if the pseudomeasurements are not critical, but redundant, the arbitrary weights assigned to them can lead to largely biased results. For this reason, transformer impedance ratios have not been included as pseudomeasurements in the present implementation.

It is important to note that, if pseudomeasurements of the estimated parameters are not used, as in the case of the present proposal, initiating the iterative process from a flat start leads to the singularity of the Jacobian matrix at the first iteration. Certainly, all the derivatives with respect to the parameters become zero at this operating point. This problem can be easily counteracted by including the parameters in the state vector only after the first iteration [6]. This is the strategy followed by the authors in the present contribution.

V. Case Studies

A well-tested industrial power system, previously used in [17], has been adopted in these case studies to validate and analyze the proposal. The topology of the network, which includes four tap-changing transformers, together with the voltage levels are depicted in Fig. 5. The specific data of the lines, transformers and loads are summarized in Table I.

In order to generate data for the multi-snapshot scenario, the tap position of the transformers and the value of the loads are randomly assigned at each instant. All the transformers provide a voltage regulating range of $\pm 7\%$, with a regulating step, ΔU, of 1%. Thus, each p.u. turns ratio is calculated at every snapshot according to

$$a = \frac{1}{1 + \Delta U \times I}, \tag{40}$$

with I being a random integer which follows a uniform discrete distribution in the range -7 to $+7$. It is worth mentioning that, according to (2)–(7), at central taps, i.e. $a = 1$, the impedance ratio, k, has no effect on the impedance values of the π-equivalent transformer model. Thus, any snapshot with one or more transformers operating at the central tap positions does not aid in the estimation of the impedance ratio of those particular machines. However, provided that there is not a transformer in the grid permanently connected at the central tap position (i.e. during the T snapshots considered in the problem), the measurement sets include information on every transformer impedance ratio, and thus, all those parameters become observable. The diversity of each snapshot is further guaranteed by assigning random values to each active and reactive power injection. Thus, a random value from a continuous uniform distribution within the range of -50% to $+50\%$ is added to the mean value of each of the loads shown in Table I. In this way, the case studies presented in this section incorporate the possible influence of the variation of

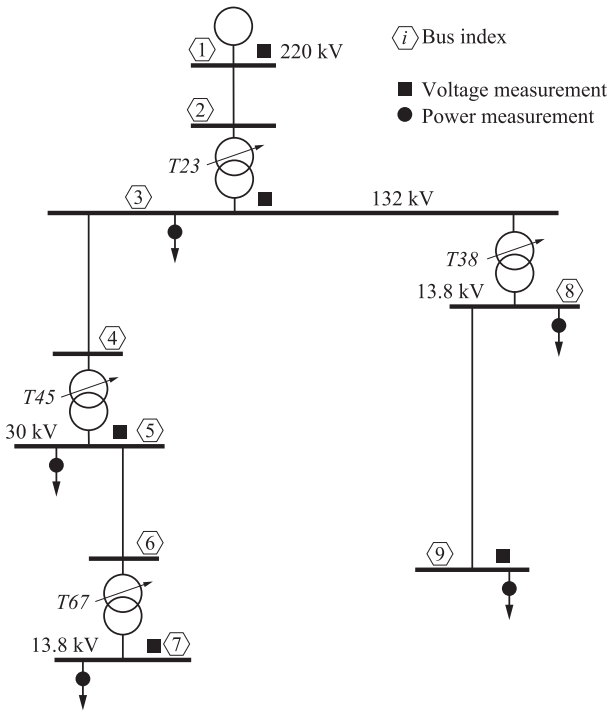

Fig. 5. 9-bus test grid. The specific set of measurements used in the case study shown in Section V-D are highlighted in this figure.

TABLE I
Parameters of the 9-Bus Test Grid

Line Data

From bus	To bus	Length [km]	Impedance [Ω/km]
1	2	4.7	$0.025 + 0.240i$
3	4	1.5	$0.161 + 0.151i$
5	6	0.3	$0.568 + 0.133i$
8	9	1.8	$0.161 + 0.112i$

Transformer Data

No.	a-range[1] [p.u.]	Rating[2] [MVA]	R_{sc} [%]	X_{sc} [%]	k [p.u.]
T23	0.934 : 1.075	2×270	0.90	12.97	0.75
T45	0.934 : 1.075	3×37.5	0.90	8.95	1.25
T67	0.934 : 1.075	10	0.95	4.76	0.70
T38	0.934 : 1.075	3×50	0.92	7.95	1.35

Load Data - Mean values[3]

Bus	P [MW]	Q [Mvar]	Bus	P [MW]	Q [Mvar]
3	84.0	26.0	8	52.0	39.0
5	34.0	12.0	9	1.7	1.5
7	7.5	5.0	–	–	–

[1] Taps are randomly selected within this range.
[2] Preceded by the number of transformers connected in parallel.
[3] Load data are randomly generated around the mean values.

TABLE II
COMPARISON OF ACTUAL AND ESTIMATED IMPEDANCE RATIOS - FULL REDUNDANCY - 20 SNAPSHOTS

Transformer p.u. Impedance Ratios			
No.	k^{AC} [p.u.]	k^{SE} [p.u.]	$\|e\|$ [%]
T23	0.7500	0.7396	1.04
T45	1.2500	1.2471	0.29
T67	0.7000	0.6994	0.06
T38	1.3500	1.3306	1.94

the transformer load level in the performance of the parameter estimation algorithm.

With the aim of emulating the measurement acquisition process, the topological information and assigned values for taps and loads were used to conduct a power flow of the grid for each snapshot. The system states, which were verified with OpenDSS [18], were used to calculate the full set of ideal measurements: bus voltages magnitudes, active and reactive power injections and active and reactive line power flows. Eventually, Gaussian noise was added to these measurements in order to obtain a set of corrupted regular measurements which, together with virtual measurements (from zero injection buses), were included in the SE process. According to [6], sensible values for the standard deviation of the measurements can be selected as $\sigma = 0.1 \cdot \gamma \cdot FS$ for voltage measurements and as $\sigma = \gamma \cdot FS$ for power measurements, where γ stands for the accuracy class of the measurement device and FS stands for the full scale value in accordance with the largest magnitude expected at the respective measurement point. In the present proposal, devices of accuracy class 0.1 according to [19] were considered and, for the sake of simplicity, the value of the corresponding ideal measurement was adopted as the full scale value.

A. Validation of the Proposal

For an initial validation of the proposal, a full redundancy scenario is considered. This includes measurements for bus voltage magnitudes, sending and receiving branch power flows, and power injections at each bus (except for bus 1 that is taken as the slack). According to (38), a redundancy of 3.35 corresponds to this base case. However, considering (39), the inclusion of k parameters in a single-snapshot implementation of the augmented SE problem reduces the redundancy level to 2.71. To recover most of the redundancy of the base case, 20 snapshots are considered in this initial study, which, according to (39), increases its level to 3.31. In this full redundancy scenario, the algorithm converges in 7 iterations using a threshold of $1e-8$ for the maximum absolute value of the state variable deviations, Δx. The conventional state variables, not shown here for space constraints, are found to be very close to the actual values, previously obtained from the power flow analysis. Finally, the estimated values of the transformer p.u. impedance ratios, k^{SE}, are presented in Table II, together with their actual values, k^{AC}, and absolute errors, $|e|$. A maximum absolute error (MAE) of 1.94% and an average absolute error (AAE) of 0.83% allow to demonstrate the validity of the proposal.

TABLE III
COMPARISON OF ESTIMATION ERRORS IN STATE VARIABLES - A) USING AN EDUCATED GUESS, $k_t = 1$, B) USING ESTIMATES OF k_t

	σ^2_{av}	$MAE(V), [\%]$	$MAE(\theta), [deg.]$
Case A	1.2776 e-4	0.0438	0.0449
Case B	0.0106 e-4	0.0078	0.0049

B. Improvement in SE Results

In [4], [5], through several case studies, the advantages of using the new transformer model with an educated guess of $k = 1$, was established. However, as the present proposal allows for the offline estimation of accurate values of transformer p.u. impedance ratios, it is interesting to assess the expected improvement in the accuracy of SE results, as those provided by an online state estimator, as a consequence of this refinement. With this aim, a single snapshot standard WLS augmented matrix state estimator was used to calculate the state variables of the grid in Fig. 5 for the 20 measurement snapshots considered in the previous case study (i.e. the one shown in subSection V-A). This test was carried out with two different setups of the transformer impedance ratios: Case A) uses the educated guess proposed in [4], [5], i.e. all the parameters are assumed as equal to 1; conversely, in Case B) the estimated parameters shown in the 3rd column of Table II were used along the SE process.

As it is highlighted in [4], [5], the errors derived from the use of an inaccurate value of k become more significant at extreme tap positions and are highly dependent on the power factor of the power flow. As the case study reported in subSection V-A uses both load values and tap positions randomly generated, a diverse influence of the errors caused by k is assured. Two figures of merit have been used to assess the comparison: (1) the MAE of bus voltage magnitudes and phase angles with respect to the true state, calculated considering the full set of buses and snapshots, and (2), the average value of the sum of variances over Q snapshots, defined as

$$\sigma^2_{av} = \frac{1}{Q}\sum_{q=1}^{Q}\left[\frac{1}{S}\sum_{s=1}^{S}\left(\hat{x}_{sq} - x_{sq}\right)^2\right], \tag{41}$$

with $\hat{x}_{sq}$ and x_{sq} being the estimated and true state of the s-th state variable of the system at snapshot q, which has been used with this aim in similar studies [20]. The true state of the system was previously obtained for each snapshot by using a power flow algorithm with the true values of k, i.e, those shown in the 2nd column of Table II. The results in Table III show the values of the aforementioned figures of merit.

From Table III, it becomes evident that the errors in the estimated states are significantly reduced with the use of accurate estimates of transformer impedance ratios. This result ensures the practical usefulness of the proposal.

C. Influence of the Number of Snapshots

As it is stated in (39), using a large number of snapshots should return the redundancy of the SE problem close to the one from the base case. However, it is still interesting to analyze if

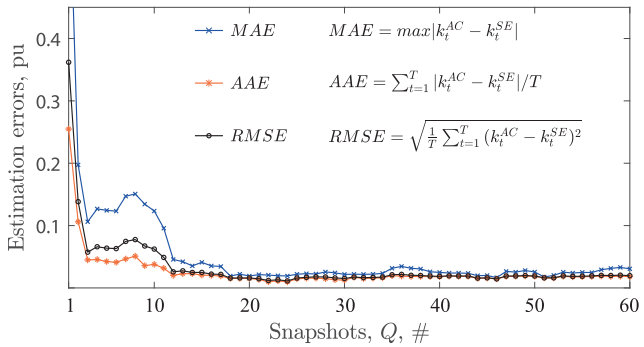

Fig. 6. Estimation errors of transformer impedance ratios vs. number of snapshots - full redundancy.

the quality of the estimates of the transformer impedance ratios keeps improving with the number of snapshots or if, from a certain point, adding more snapshots is not really worthy. This case study is designed to test this specific feature, and for that, the same base case of subSection V-A is used. However, now, the test is repeated with an increasing number of snapshots, Q, ranging from 1 to 60. The quality of these multi-snapshot estimates is assessed by using different figures of merit. Thus, Fig. 6 represents the value of the MAE, AAE and root mean square error (RMSE). The definitions of these figures of merit, in the context of this test, are included in the legend of the figure. Note that k_t^{AC} and k_t^{SE} are the actual and estimated values of p.u. impedance ratios, t, and T being the particular and the total number of transformer impedance ratios to be estimated.

From Fig. 6, it can be concluded that using a very low number of snapshots is not feasible, as Q in ranges from 1 to 11 may lead to gross errors in the estimation of the parameters. On the other hand, the graph shows that these errors decline very fast as new information is included into the problem by increasing the number of snapshots. In this case study, the MAE is always lower than 5% when 12 or more snapshots are included into the problem, and lower than 3.5% if Q is raised to 17. Regarding the RMSE, it is always lower than 5% if at least 11 snapshots are used and lower than 3.5% if more than 12 snapshots are included. Similarly, 9 and 11 snapshots are enough to assure an AAE under 5% and 3.5%, respectively.

It is also interesting to note that, from a certain number of Q, the benefit of adding new snapshots is only marginally significant. Thus, none of the p.u. impedance ratio estimation shows an error higher than 5% (compared with the actual values) when the number of snapshots included in the problem is at least 20. This comparison is presented in Table IV. In any case, a compromise between accuracy and computational burden should be assumed by the user.

D. Influence of the Redundancy Level

An interesting concern related to the utilisation of the proposed methodology, is to analyze the influence of the redundancy level on its capability to provide accurate estimates of the transformer impedance ratios. With this aim, the base case used in Section V-A is downgraded now by removing some of

TABLE IV
COMPARISON OF ACTUAL AND ESTIMATED VALUES - FULL REDUNDANCY - DIFFERENT SNAPSHOTS

Transformer p.u. Impedance Ratios					
		$Q = 20$		$Q = 60$	
No.	k^{AC} [p.u.]	k^{SE} [p.u.]	$\|e\|$ [%]	k^{SE} [p.u.]	$\|e\|$ [%]
T23	0.7500	0.7429	0.71	0.7354	1.46
T45	1.2500	1.2309	1.91	1.2194	3.06
T67	0.7000	0.6812	1.88	0.6889	1.11
T38	1.3500	1.3342	1.57	1.3333	1.67

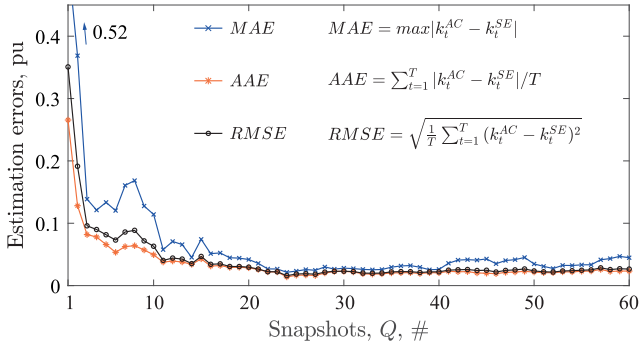

Fig. 7. Estimation errors of transformer impedance ratios vs. number of snapshots - minimum redundancy.

the measurements, down to the point in which the system is just observable with a single snapshot. In this minimum redundancy case study, the 17 state variables and 4 parameters to be estimated in the single snapshot scenario, are obtained from a set of 21 measurements, thus leading, according to (39), to a redundancy level of 1 for a single-snapshot implementation, i.e. $\varepsilon_1 = 1$. Specifically, all the power flow measurements, less common at certain parts of the grid, have been completely removed. On the other hand, 5 of the 9 bus voltage magnitudes as well as the full set of power injection measurements are retained. For the benefit of the reader, the specific set of measurements considered in the problem is depicted in Fig. 5.

The same multi-snapshot analysis previously conducted in Section V-C for the full redundancy case, has been carried out here for the new minimum redundancy scenario. Fig. 7 shows the values of the different figures of merit, i.e. MAE, AAE and RMSE for the different number of snapshots included into the problem, ranging from 1 to 60. Thus, according to (39), the maximum redundancy level considered along the test is limited to $\varepsilon_{60} = 1.23$.

As it can be seen in Fig. 7, a similar pattern to the one derived from the full redundancy scenario is obtained, though slightly higher errors arise in this case. However, it is important to highlight that the convergence ratio of the problem is not deteriorated and not more than 8 iterations are needed to solve the SE for any value of Q. This is an important observation for those parts of the grid where full redundancy is typically far from the reality of standard infrastructures. Specifically, the MAE needs at least 18 snapshots to drop under 5%. For the case of the RMSE, 11 snapshots are needed to go under this error threshold. Finally,

TABLE V
COMPARISON OF ACTUAL AND ESTIMATED VALUES - MINIMUM REDUNDANCY - DIFFERENT SNAPSHOTS

Transformer p.u. Impedance Ratios					
		$Q = 30$		$Q = 60$	
No.	k^{AC} [p.u.]	k^{SE} [p.u.]	$\|e\|$ [%]	k^{SE} [p.u.]	$\|e\|$ [%]
T23	0.7500	0.7735	2.35	0.7626	1.26
T45	1.2500	1.2220	2.80	1.2052	4.48
T67	0.7000	0.6779	2.21	0.6841	1.59
T38	1.3500	1.3324	1.76	1.3301	1.99

just 10 snapshots are enough to reduce the AAE under 5%. Estimations from specific snapshots are presented in Table V for the minimum redundancy case. This allows to conclude that, in order to achieve similar accuracy levels, the user should be aware of including a higher number of snapshots when redundancy is compromised. Indeed, this observation is aligned with the nature of the problem, as fewer information about the system is being provided if this compensation is not conducted.

E. Influence of Bad Data

As it was stated in Section IV-C, the proposed parameter estimation algorithm is designed to work offline, and thus, a conventional online state estimator is responsible for the detection, identification and removal of bad data. However, using inaccurate values of the transformer impedance ratios (as during the initialization process in which an educated guess is used, $k = 1$), can lead the online state estimator to erroneously flag and remove measurements as bad data. The present case study analyses if the removal of these measurements from the data set could have a significant influence on the estimation of transformer impedance ratios by the offline algorithm.

To replicate the performance of an online state estimator, a single snapshot standard WLS augmented matrix algorithm was applied to the 60 snapshots considered in the full redundancy case study analysed in Section V-C. A value of $k = 1$ was assigned to the impedance ratio of each of the four tapped transformers in Fig. 5. The normalized residual test, with a threshold level of 4, was used to detect, identify and remove bad data. The estimation process and bad data test are sequentially repeated until the complete filtering of the input data. As a result, bad data was identified in 28 of the 60 snapshots. Up to a maximum of 4 measurements had to be removed from a single snapshot to reach a set of fully filtered data.

The parameter estimation algorithm proposed in this work was applied to the filtered set of measurements for an increasing number of snapshots (from 1 to 60). Fig. 8 compares the value of the average absolute error of the estimated parameters with those obtained in Section V-C. As can be observed in Fig. 8, the removal of measurements can lead to a slight increase in parameter estimation errors when a low number of snapshots are used as input data. However, this effect is practically obliterated by the addition of more snapshots.

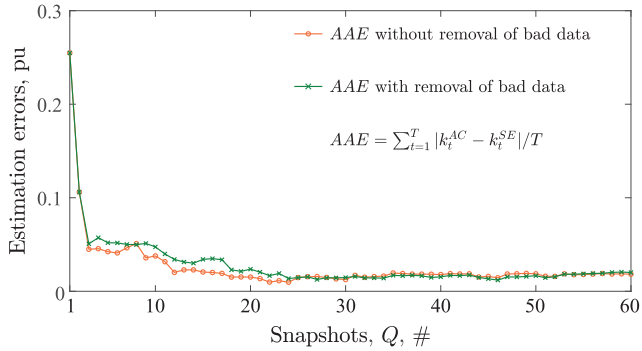

Fig. 8. Estimation errors of transformer impedance ratios vs. number of snapshots - influence of bad data.

It is important to highlight that this situation is only expected during the first execution of the algorithm in a particular grid. Once a realistic approximation to the values of k is available for the online estimator, erroneous bad data detections due to transformer model inaccuracies are not likely to occur. Thus, using a larger number of snapshots during the initialization can be considered a sensible recommendation.

Finally, in a context of lower redundancy, the same pattern shown in Section V-D is expected. Notice that if the removal of bad data causes the loss of observability, the corresponding snapshot would just not be provided by the online estimator, and thus, it will not have any influence on the parameter estimation algorithm.

VI. CONCLUSION

An offline state-vector-augmented parameter estimation method, capable of providing accurate estimates of transformer impedance ratios, is proposed, validated, and analyzed in this work. Moreover, the derivatives of the different measurement functions in terms of the new parameter, which are essential for this or any other linearized state estimator, are provided as a contribution. This study, calls attention to the hindrances found in the estimation of these parameters, such as the significantly lower sensitivity of the measurement functions with respect to p.u. impedance ratios and the reduction of redundancy that their inclusion causes in the state estimation problem. To overcome these difficulties, the authors propose a method based on the use of a multi-snapshots scenario. A set of case studies are presented in order to validate and demonstrate the usefulness of the proposal, including an analysis of the effect of the number of snapshots and the redundancy level on the accuracy of the estimation. They allow to conclude that, a lower number of snapshots, in the range 1 to 10, are not enough to derive accurate results regardless of the redundancy level. However, the inclusion of a higher number of snapshots always allows to reach acceptable estimates. Though a low measurement redundancy level requires a higher number of snapshots to reach the same accuracy, this work demonstrates that even those systems close to the limit of observability can be handled successfully by the proposed algorithm.

REFERENCES

[1] J. D. Glover, M. S. Sarma, and T. Overbye, *Power System Analysis and Design.*, 5th ed., Boston, MA, USA: Cengage Learning, 2012.

[2] Powerworld User's Guide, 2011. [Online]. Available: http://www.powerworld.com.

[3] L. V. Barboza, H. Zurn, and R. Salgado, "Load tap change transformers: A modeling reminder," *IEEE Power Eng. Rev.*, vol. 21, no. 2, pp. 51–52, Feb. 2001.

[4] J. M. Cano, M. R. R. Mojumdar, and G. A. Orcajo, "Reconciling tap-changing transformer models," *IEEE Trans. Power Del.*, vol. 34, no. 6, pp. 2266–2268, Dec. 2019.

[5] J. M. Cano, M. R. R. Mojumdar, and G. A. Orcajo, "On the consistency of tap-changing transformer models in power system studies," in *Proc. IEEE Power Energy Soc. Gen. Meeting*., 2020, pp. 1–5.

[6] A. Abur and A. G. Exposito, *Power System State Estimation: Theory and Implementation*. Boca Raton, FL, USA: CRC Press, 2004.

[7] A. Monticelli, *State Estimation in Electric Power Systems: A Generalized Approach*. Berlin, German: Springer Science & Business Media, 2012.

[8] O. Alsac, N. Vempati, B. Stott, and A. Monticelli, "Generalized state estimation," *IEEE Trans. Power Syst.*, vol. 13, no. 3, pp. 1069–1075, Aug. 1998.

[9] M. Castillo, J. London Jr, and N. Bretas, "Identification and estimation of power system branch parameter error," in *Proc. IEEE Power Energy Soc. Gen. Meeting*, 2009, pp. 1–8.

[10] P. A. Teixeira, S. R. Brammer, W. L. Rutz, W. Merritt, and J. Salmonsen, "State estimation of voltage and phase-shift transformer tap settings," *IEEE Trans. Power Syst.*, vol. 7, no. 3, pp. 1386–1393, Aug. 1992.

[11] Y. Lin and A. Abur, "Enhancing network parameter error detection and correction via multiple measurement scans," *IEEE Trans. Power Syst.*, vol. 32, no. 3, pp. 2417–2425, May 2017.

[12] Y. Lin and A. Abur, "Robust state estimation against measurement and network parameter errors," *IEEE Trans. Power Syst.*, vol. 33, no. 5, pp. 4751–4759, Sep. 2018.

[13] G. N. Korres, P. J. Katsikas, and G. C. Contaxis, "Transformer tap setting observability in state estimation," *IEEE Trans. Power Syst.*, vol. 19, no. 2, pp. 699–706, May 2004.

[14] P. Zarco and A. G. Exposito, "Power system parameter estimation: A survey," *IEEE Trans. Power Syst.*, vol. 15, no. 1, pp. 216–222, Feb. 2000.

[15] F. Aschmoneit, N. Peterson, and E. Adrian, "State estimation with equality constraints," in *Proc. 10th PICA Conf.*, 1977, pp. 427–430.

[16] A. Gjelsvik, S. Aam, and L. Holten, "Hachtel's augmented matrix method-a rapid method improving numerical stability in power system static state estimation," *IEEE Trans. Power App. Syst.*, vol. PAS-104, no. 11, pp. 2987–2993, Nov. 1985.

[17] M. R. R. Mojumdar, J. M. Cano, S. Jaman, and G. A. Orcajo, "Smoothing parameter optimization routine for high-quality a priori estimates in forecasting-aided state estimation," in *Proc. IEEE Power Energy Soc. Gen. Meeting*, 2018, pp. 1–5.

[18] R. C. Dugan and D. Montenegro, "Open distribution system simulator (OpenDSS): Reference guide," *Elect. Power Res. Inst.*, Inc., Knoxville, TN, Jun. 2019. [Online]. Available: https://sourceforge.net/p/electricdss/wiki/Home/

[19] *Electricity Meters, 0.1, 0.2 and 0.5 Accuracy Classes*. ANSI C12. 20.2015, American National Standards Institute, Washington, D.C., Standard, 2015.

[20] S. Chakrabarti, E. Kyriakides, G. Ledwich, and A. Ghosh, "Inclusion of PMU current phasor measurements in a power system state estimator," *IET Gener., Transmiss. Distrib.*, vol. 4, no. 10, pp. 1104–1115, 2010.

Md Rejwanur R. Mojumdar (Graduate Student Member, IEEE) received the Joint M.Sc. degree in 2014 from the Erasmus Mundus Master Course in Sustainable Transportation and Electrical Power Systems (EMMC STEPS). He is currently working toward the Ph.D. degree from the University of Oviedo, Spain. He started as a SCADA Engineer for AREVA T&D. Then he was in several research positions with the University of Oviedo, Spain, University of Stavanger, Norway, and INESC TEC, Portugal. In 2020, he joined the Electrical Control System Department, ABB AS, Norway. His research interests include the state estimation, modeling and algorithms for power management systems, distributed generation and smart grids.

José M. Cano (Senior Member, IEEE) received the M.Sc. and Ph.D. degrees in electrical engineering from the University of Oviedo, Spain, in 1996 and 2000, respectively. In 1996, he joined the Department of Electrical Engineering, University of Oviedo, Spain, where he is currently a Full Professor. During 2012 and 2014, he was a Visiting Associate Professor with the Department of Electrical and Computing Engineering, University of British Columbia, Canada. His main research interests include power quality solutions for industry, power converters, power system state estimation, distributed generation and smart grids.

Gonzalo A. Orcajo (Member, IEEE) was born in Gijón, Spain, in 1965. He received the M.Sc. and Ph.D. degrees in electrical engineering from the University of Oviedo, Spain, in 1990 and 1998, respectively. In 1992, he joined the Department of Electrical Engineering, University of Oviedo, where he is currently an Associate Professor. His main research interests include power quality in industrial power systems. In recent years, he has focused on the detection and location of faults in distribution systems and on reactive power compensation systems.